1521-0111/12/8204-636–644$25.00
MOLECULAR PHARMACOLOGY
Vol. 82, No. 4
77099/3794023

Mol Pharmacol 82:636–644, 2012

P-Glycoprotein, Multidrug-Resistance Associated Protein 2, Cyp3a, and Carboxylesterase Affect the Oral Availability and Metabolism of Vinorelbine[S]

Jurjen S. Lagas, Carola W. N. Damen, Robert A. B. van Waterschoot, Dilek Iusuf, Jos H. Beijnen, and Alfred H. Schinkel

Division of Molecular Oncology (J.S.L., R.A.B.v.W., D.I., A.H.S.), The Netherlands Cancer Institute, Amsterdam, The Netherlands; and Department of Pharmacy and Pharmacology, Slotervaart Hospital, Amsterdam, the Netherlands (J.S.L., C.W.N.D., J.H.B.)

Received December 5, 2011; accepted July 5, 2012

ABSTRACT

We investigated the interactions of the anticancer drug vinorelbine with drug efflux transporters and cytochrome P450 3A drug-metabolizing enzymes. Vinorelbine was transported by human multidrug-resistance associated protein (MRP) 2, and Mrp2 knockout mice displayed increased vinorelbine plasma exposure after oral administration, suggesting that Mrp2 limits the intestinal uptake of vinorelbine. Using P-glycoprotein (P-gp), Cyp3a-, and P-gp/Cyp3a knockout mice, we found that the absence of P-gp or Cyp3a resulted in increased vinorelbine plasma exposure, both after oral and intravenous administration. Surprisingly, P-gp/Cyp3a knockout mice displayed markedly lower vinorelbine plasma concentrations than wild-type mice upon intravenous administration but higher concentrations upon oral administration. This could be explained by highly increased formation of 4′-*O*-deacetylvinorelbine, an active vinorelbine metabolite, especially in P-gp/Cyp3a knockout plasma. Using wild-type and Cyp3a knockout liver microsomes, we found that 4′-*O*-deacetylvinorelbine formation was 4-fold increased in Cyp3a knockout liver and was not mediated by Cyp3a or other cytochrome P450 enzymes. In vitro incubation of vinorelbine with plasma revealed that vinorelbine deacetylation in Cyp3a and especially in P-gp/Cyp3a knockout mice but not in P-gp-deficient mice was strongly up-regulated. Metabolite formation in microsomes and plasma could be completely inhibited with the nonspecific carboxylesterase (CES) inhibitor bis(4-nitrophenyl) phosphate and partly with the CES2-specific inhibitor loperamide, indicating that carboxylesterase Ces2a, which was appropriately up-regulated in Cyp3a and especially in P-gp/Cyp3a knockout liver was responsible for the 4′*O*-deacetylvinorelbine formation. Such compensatory up-regulation can complicate the interpretation of knockout mouse data. Nonetheless, P-gp, Mrp2, Cyp3a, and Ces2a clearly restricted vinorelbine availability in mice. Variation in activity of their human homologs may also affect vinorelbine pharmacokinetics in patients.

Introduction

Vinorelbine is a semisynthetic vinca alkaloid that is indicated in the treatment of non-small-cell lung cancer and advanced breast cancer (Domenech and Vogel, 2001; Gralla et al., 2007). In current clinical practice, vinorelbine is mainly intravenously applied despite the development of an oral vinorelbine formulation, which has been approved in several European countries. This may be explained by the relatively high interindividual variability in drug exposure that was observed for oral vinorelbine administration in numerous clinical studies (Gralla et al., 2007; Hirsh et al., 2007; Rossi et al., 2007; Delord et al., 2009). For clinical practice, it is thus important to identify interactions of vinorelbine with drug efflux transporters and drug-metabolizing enzymes because these systems might affect the exposure and toxicity of vinorelbine, especially upon oral administration. Moreover, drug efflux transporters may also directly contribute to resistance of tumors against vinorelbine.

It has been well established by various groups that the drug efflux transporter P-glycoprotein (MDR1/ABCB1) transports vinorelbine in vitro and mediates resistance against vinorelbine (Adams and Knick, 1995; Takara et al.,

Article, publication date, and citation information can be found at http://molpharm.aspetjournals.org.
http://dx.doi.org/10.1124/mol.111.077099.
[S] The online version of this article (available at http://molpharm.aspetjournals.org) contains supplemental material.

ABBREVIATIONS: MRP, multidrug-resistance associated protein; ABCC, ATP-binding cassette transporter family C; P-gp, P-glycoprotein; AUC, under the plasma concentration-time curve; BNPP, bis(4-nitrophenyl) phosphate; MDCK, Madin-Darby canine kidney; LC, liquid chromatography; MS/MS, tandem mass spectrometry; P450, cytochrome P450; CES, carboxylesterase; RT, reverse transcriptase; PCR, polymerase chain reaction.

2002; Shepard et al., 2003). However, data about the in vivo interaction of vinorelbine with P-gp are inconclusive. For instance, Press et al. (2006) found no significant changes in oral or intravenous vinorelbine area under the plasma concentration-time curves (AUCs) between wild-type (WT) or P-gp-deficient [*Mdr1a/1b*(−/−)] mice, although interindividual variation in these experiments was very high, potentially obscuring modest shifts. Furthermore, in a phase I study in 26 patients with advanced solid tumors, the P-gp inhibitor tariquidar was combined with intravenously applied vinorelbine (20 mg/m^2), but alterations in the pharmacokinetics of vinorelbine were not observed (Abraham et al., 2009). On the other hand, Wong et al. (2006) found in a cohort of 41 patients receiving intravenous vinorelbine that low hepatic ^{99m}Tc-hexakis-2-methoxybutylisonitrile clearance (used as a measure for P-gp-mediated clearance) significantly correlated with low vinorelbine clearance. In addition, a phase I trial with 19 patients with advanced solid tumors revealed increased exposure and decreased clearance when intravenous vinorelbine (22.5 mg/m^2) was combined with the potent P-gp inhibitor zosuquidar (Lê et al., 2005). A more extensive analysis of in vivo vinorelbine-P-gp interactions thus seemed worthwhile.

To date, interactions of vinorelbine with the drug efflux transporter MRP2 (ABCC2) have not been reported. However, cellular resistance to the vinca alkaloid vincristine has been associated with MRP2 expression (Chen et al., 1999; Kawabe et al., 1999), and in vitro transport of vinblastine by MRP2 has also been demonstrated (Evers et al., 1998, 2000a; Huisman et al., 2005). It thus seemed possible that vinorelbine might also be transported by MRP2, which could affect vinorelbine pharmacokinetics, toxicity, and resistance of tumors.

Vinorelbine is thought to be mainly metabolized by CYP3A4 to inactive metabolites (Kajita et al., 2000; Beulz-Riche et al., 2005). However, to some extent vinorelbine is also converted to a pharmacodynamically active metabolite, 4′-*O*-deacetylvinorelbine. In fact, metabolic profiling after oral vinorelbine administration revealed that 4′-*O*-deacetylvinorelbine is the predominant metabolite in human blood with an elimination half-life of at least 100 h (Marty et al., 2001). This deacetylation reaction is believed to be catalyzed by carboxylesterase enzymes, which are formed in the liver and reside in blood, although specific enzyme(s) responsible for this activity have not been identified yet (Beulz-Riche et al., 2005; Delord et al., 2009).

The aim of this study was to obtain better insight into the potential impact of P-gp, MRP2, and CYP3A on the pharmacokinetics of vinorelbine, using in vitro, ex vivo, or in vivo assays and P-gp-, Mrp2-, and Cyp3a-deficient mouse strains.

Materials and Methods

Chemicals. Vinorelbine (Navelbine) 10 mg/ml concentrate for solution for infusion originated from Pierre Fabre Medicament (Boulogne, France). Vinorelbine tartrate was purchased from Sequoia Research Products (Pangbourne, UK). Deacetylvinblastine sulfate was obtained from the Faculty of Pharmacy (University of Utrecht, Utrecht, The Netherlands). Loperamide hydrochloride and bis(4-nitrophenyl) phosphate (BNPP) were from Sigma-Aldrich (Steinheim, Germany). Methoxyflurane (Metofane) was from Medical Developments Australia (Springvale, VIC, Australia). Heparin (5000 IU/ml) was from Leo Pharma BV (Breda, The Netherlands). The organic solvents methanol, acetonitrile (both high-performance liquid chromatography-grade), and diethyl ether were from Merck (Darmstadt, Germany). Drug-free human plasma was from healthy volunteers. GlaxoSmithKline (Uxbridge, UK) kindly provided elacridar (GF120918). All other chemicals and reagents were obtained from Sigma-Aldrich.

Transport Assays. Polarized canine kidney MDCK-II cell lines were used in transport assays. MDCK-II cells transduced with human MRP2 were described previously (Evers et al., 1998). Transepithelial transport assays using Transwell plates were performed as described previously with minor modifications (Schinkel et al., 1995). Experiments were performed in the presence of 5 μM elacridar to inhibit any endogenous P-glycoprotein activity. Elacridar at 5 μM does not affect MRP2 activity (Evers et al., 2000b). Elacridar was present in both compartments during a 2-h preincubation and during the transport experiment. After preincubation, experiments were started (t = 0) by replacing the medium in either the apical or basolateral compartment with fresh OptiMEM medium, either with or without 5 μM Elacridar and containing 5 μM vinorelbine. Cells were incubated at 37°C in 5% CO_2, and 50-μl aliquots were taken at t = 2 and 4 h. The samples were diluted with 450 μl of drug-free human plasma, 50 μl of internal standard (100 ng/ml deacetylvinblastine) was added, and the samples were extracted with 3 ml of diethyl ether. Vinorelbine was quantified by high-performance liquid chromatography, as described previously (van Tellingen et al., 1992). Transport was calculated as the fraction of drug found in the acceptor compartment relative to the total amount added to the donor compartment at t = 0. Transport is given as mean percentage ± S.D. (n = 3). Membrane tightness was assessed in parallel, using the same cells seeded on the same day and at the same density, by analyzing transepithelial [^{14}C]inulin (approximately 3 kBq/well) leakage. Leakage had to remain <2% of the total added radioactivity per 2 h. Active transport across MDCK-II monolayers was expressed by the relative transport ratio (r), defined as percentage of apically directed translocation divided by percentage of basolaterally directed translocation after 4 h (Huisman et al., 2005). The apparent permeability coefficient (P_{app}) was calculated using the equation P_{app} (centimeters per second) = $dC/dt \cdot 1/A \cdot V/C_0$ (centimeters per second), where dC/dt (micromoles per second) represents the flux across the monolayer (permeability rate), A (square centimeters) represents the surface area of the monolayer, V (cubic centimeters) represents the volume of the receiver chamber, and C_0 (micromolar concentration) represents the initial concentration in the donor compartment (Irvine et al., 1999).

Animals. Mice were housed and handled according to institutional guidelines complying with Dutch legislation. Animals used in this study were female *Mdr1a/1b*(−/−) (Schinkel et al., 1997), *Mrp2*(−/−) (Vlaming et al., 2006), *Cyp3a*(−/−) (van Herwaarden et al., 2007), *Mdr1a/1b/Cyp3a*(−/−) (van Waterschoot et al., 2009), and WT mice, all of a >99% FVB genetic background, between 9 and 12 weeks of age. Animals were kept in a temperature-controlled environment with a 12-h light/12-h dark cycle and received a standard diet (AM-II; Hope Farms, Woerden, The Netherlands) and acidified water ad libitum.

Plasma Pharmacokinetics. For oral studies, vinorelbine (10 mg/ml) was 10-fold diluted with saline and dosed at 10 mg/kg b.wt. (10 ml/kg). To minimize variation in absorption, mice were fasted for 3 h before vinorelbine was administered by gavage into the stomach, using a blunt-ended needle. Multiple blood samples (~40 μl) were collected from the tail vein at 15 and 30 min and 1, 2, 4, 8, and 24 h, using heparinized capillary tubes (Oxford Labware, St. Louis, MO). Blood samples were centrifuged at 2100 × g for 6 min at 4°C, and the plasma was completed to 200 μl with drug-free human plasma and stored at −20°C until analysis. For intravenous studies, vinorelbine (10 mg/ml) was diluted 5-fold with saline and injected as single bolus at 10 mg/kg (5 ml/kg) into the tail vein. Blood samples were collected by cardiac puncture under methoxyflurane anesthesia at 7.5 and 30 min and 1, 2, 4, 8 and 24 h, with four animals per time point.

Samples were processed as described above and stored at −20°C until analysis.

Drug Analysis in Plasma. Plasma concentrations of vinorelbine and 4′-*O*-deacetylvinorelbine were determined by LC-MS/MS as described previously (Damen et al., 2009).

Pharmacokinetic Calculations and Statistical Analysis. The AUC was calculated using the trapezoidal rule. The peak plasma concentration (C_{max}) and the time of maximum plasma concentration (T_{max}) were estimated from the original data. Plasma clearance (CL) after intravenous administration was calculated by the formula CL = dose/AUC. The oral bioavailability (F) was calculated by the formula $F = AUC_{oral}/AUC_{i.v.} \times 100\%$. To assess statistical significance, the two-sided unpaired Student's t test (two groups) or one-way analysis of variance followed by Dunnett's multiple comparison test (>2 groups) was performed. Data obtained with single and combination knockout mice were compared with data obtained with WT mice, unless stated otherwise. Data are presented as means ± S.D., and differences were considered statistically significant when $P < 0.05$.

Microsomal Incubations. Microsomes from the livers of WT and *Cyp3a*(−/−) mice were prepared as described previously (Emoto et al., 2000). Incubations were performed in triplicate at 37°C in a total volume of 200 μl, containing 100 mM potassium phosphate buffer (pH 7.4), an NADPH-regenerating system (BD Biosciences, San Diego, CA). and 0.5 mg of protein/ml liver microsomes. Reactions were started by addition of vinorelbine (18.5 μM), allowed to proceed for 20 min, and terminated by addition of 100 μl of ice-cold acetonitrile. Control incubations omitting cofactor NADPH were performed to establish whether the metabolism was P450-dependent. For inhibition experiments, the nonspecific CES inhibitor BNPP (100 μM), the CES2-specific inhibitor loperamide (100 μM), or vehicle was preincubated for 5 min at 37°C, and reactions were started by addition of vinorelbine (18.5 μM). Incubations were performed without NADPH, allowed to proceed for 30 min, and terminated by addition of 100 μl of ice-cold acetonitrile. Concentrations of vinorelbine and 4′-*O*-deacetylvinorelbine in supernatant (6800*g* for 10 min) were determined by LC-MS/MS (Damen et al., 2009).

Plasma Incubations. Blood was collected from WT, *Mdr1a/1b*(−/−) (Schinkel et al., 1997), *Cyp3a*(−/−) (van Herwaarden et al., 2007), and *Mdr1a/1b/Cyp3a*(−/−) (van Waterschoot et al., 2009) mice (n = 4/strain) by cardiac puncture under methoxyflurane anesthesia. Blood samples were immediately centrifuged at 2100*g* for 6 min at ambient temperature, and plasma was collected. Plasma samples (390 μl) were warmed to 37°C, and incubations were started by addition of 10 μl of vinorelbine stock solution (260 μM) to obtain a final concentration of 6.5 μM. Samples of 25 μl were collected at 0, 15, 30, 60, and 120 min. For inhibition experiments, the nonspecific CES inhibitor BNPP (100 μM), the CES2-specific inhibitor loperamide (100 μM), or vehicle was preincubated for 5 min at 37°C. Reactions were started by addition of vinorelbine (6.5 μM) and allowed to proceed for 120 min. Samples were immediately completed to 100 μl with ice-cold acetonitrile to stop the deacetylation reaction and subsequently stored at −20°C until analysis. Concentrations of vinorelbine and 4′-*O*-deacetylvinorelbine were determined by LC-MS/MS (Damen et al., 2009).

RNA Isolation, cDNA Synthesis, and Real-Time RT-PCR. Livers of mice between 9 and 11 weeks of age (n = 3/genotype) were excised and immediately placed in an appropriate volume of RNA*later* (QIAGEN, Venlo, The Netherlands). They were stored at 4°C until RNA was extracted using the RNeasy Mini Kit (QIAGEN) according to the manufacturer's protocol. Subsequently, cDNA was generated using 5 μg of total RNA in a synthesis reaction using random hexamers (Applied Biosystems, Foster City, CA) and SuperScript II reverse transcriptase (Invitrogen, Carlsbad, CA) according to the supplier's protocols. The reverse transcription reaction was performed for 60 min at 42°C with a deactivation step of 15 min at 70°C. cDNA was stored at −20°C until use. Real-time RT-PCR was performed using specific primers (QIAGEN) on an Applied Biosystems 7500 real-time cycler system as described previously (van Waterschoot et al., 2008). Results were analyzed by the comparative C_t method as described previously (Schmittgen and Livak, 2008), and statistical analysis was performed on ΔC_t values as described previously (Yuan et al., 2006).

Results

In Vitro Transport of Vinorelbine by MRP2. To determine whether vinorelbine (Fig. 1A) is transported by MRP2, we used polarized MDCK-II cells transduced with human MRP2 cDNA. The MDCK-II-Neo cell line was used as a control, because it contains very little endogenous canine Mrp2 (Evers et al., 1998). Because vinorelbine is a well established P-gp substrate, 5 μM elacridar was added to inhibit any transport by endogenous canine P-gp. In MDCK-II-Neo cells no active polarized transport of vinorelbine was observed, as evident from roughly equal basolateral-to-apical and apical-to-basolateral translocation rates (Fig. 1B). In contrast, in MRP2-transduced cells, apically directed translocation was markedly increased, and basolaterally directed translocation was markedly decreased (Fig. 1C). The transport ratio r, which is a measure for active transport, was 3.5-fold increased (1.3 for Neo versus 4.5 for MRP2-transduced cells) (Fig. 1). Vinorelbine is thus a transported substrate of human MRP2.

Impact of Mrp2 and P-gp on the Oral AUC of Vinorelbine. To test whether Mrp2 and P-gp restrict the oral uptake of vinorelbine, we orally administered 10 mg/kg vinorelbine to WT, *Mrp2*(−/−), and *Mdr1a/1b*(−/−) mice. Oral absorption in all strains was very rapid, and maximal plasma con-

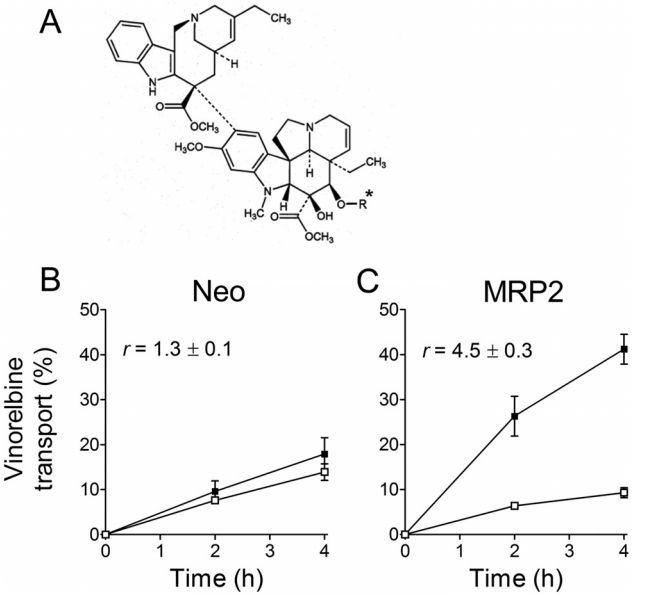

Fig. 1. Molecular structures of vinorelbine (R* = $COCH_3$) and 4′-*O*-deacetylvinorelbine (R* = H) (A) and transepithelial transport of vinorelbine (5 μM) in MDCK-II-Neo cells (B) or MDCK-II-MRP2 cells (C), in the presence of elacridar (5 μM). At t = 0 h, vinorelbine was applied in one compartment (apical or basolateral), and the percentage translocated to the opposite compartment at t = 2 and 4 h was plotted (n = 3). ■, translocation from the basolateral to the apical compartment; □, translocation from the apical to the basolateral compartment. r represents the relative transport ratio (i.e., the apically directed translocation divided by the basolaterally directed translocation) at t = 4 h. Data represent means ± S.D. At t = 4 h, 1% of transport is approximately equal to an apparent permeability coefficient (P_{app}) of 0.30 × 10^{-6} cm/s.

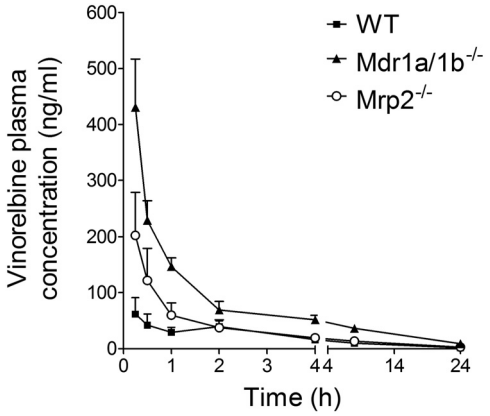

Fig. 2. Plasma concentration-time curves of vinorelbine in WT (■), *Mdr1a/1b*(−/−) (▲), and *Mrp2*(−/−) (○) mice, after oral administration of 10 mg/kg vinorelbine. Data represent mean concentrations ± S.D.; $n = 5$.

TABLE 1
Plasma pharmacokinetic parameters after oral administration of vinorelbine at 10 mg/kg
Data are means ± S.D.; $n = 5$.

	Strain		
	WT	*Mdr1a/1b*(−/−)	*Mrp2*(−/−)
AUC_{0-24}, h · mg^{-1} · l^{-1}	0.27 ± 0.04	1.00 ± 0.17*	0.41 ± 0.10*
C_{max}, mg/l	0.06 ± 0.03	0.43 ± 0.09**	0.20 ± 0.08*
T_{max}, h	0.25	0.25	0.25

*$P < 0.05$, compared with WT mice.
**$P < 0.01$.

centrations were reached before 15 min, the first sampling time point (Fig. 2). The oral AUC up to 24 h (AUC_{0-24}) in *Mrp2*(−/−) mice was 1.5-fold higher than that in WT mice ($P < 0.05$) (Fig. 2; Table 1), and the C_{max} (earliest measured time point) was 3.3-fold increased ($P < 0.05$). The oral AUC_{0-24} in *Mdr1a/1b*(−/−) mice was 3.6-fold higher than that in WT mice ($P < 0.05$) (Fig. 2; Table 1), and the C_{max} (earliest measured time point) was 7.0-fold increased ($P < 0.05$). These results show that Mrp2 can modestly and P-gp can markedly restrict the oral availability of vinorelbine. The effect of the absence of these transporters was particularly strong shortly after drug administration (15 and 30 min), suggesting a direct impact on the intestinal uptake of vinorelbine.

Impact of P-gp and Cytochrome P450 3A on Vinorelbine Plasma Pharmacokinetics. Because we had found that P-gp markedly affected the oral AUC of vinorelbine and because it is known that CYP3A4 can mediate metabolism of vinorelbine (Beulz-Riche et al., 2005), it was of interest to establish the separate and combined impact of these two detoxifying systems on vinorelbine pharmacokinetics. We previously showed that for docetaxel, also a shared P-gp and CYP3A substrate, simultaneous disruption of both systems caused a drastic increase in oral AUC (van Waterschoot et al., 2009). We therefore compared vinorelbine oral and intravenous plasma pharmacokinetics in WT, *Mdr1a/1b*(−/−), *Cyp3a*(−/−), and combination *Mdr1a/1b/Cyp3a*(−/−) mice. In line with the independent results described above, *Mdr1a/1b*(−/−) mice had a 3.4-fold higher oral AUC_{0-24} than WT mice ($P < 0.05$) (Fig. 3A; Table 2) and the C_{max}, reached within 15 min after administration, was ~10-fold higher than in WT mice ($P < 0.01$). For *Cyp3a*(−/−) mice, the oral AUC_{0-24} and C_{max} were 2.2- and 2.5-fold higher than those in WT mice, respectively ($P < 0.05$ for both parameters) (Fig. 3A; Table 2). These results indicate that both P-gp and Cyp3a reduce the oral AUC of vinorelbine. Whereas the effect of P-gp deficiency was most obvious very shortly after drug administration (15 min), for Cyp3a deficiency the strongest effect was seen only after 1 h. Unexpectedly, oral administration of vinorelbine to *Mdr1a/1b/Cyp3a*(−/−) mice did not result in an additive effect of the combined deficiencies on vinorelbine AUC. In fact, the AUC_{0-24} and the C_{max}, although still higher than those in WT mice ($P < 0.05$), were not significantly different from those observed for *Mdr1a/1b*(−/−) mice (Fig. 3A; Table 2).

After intravenous administration of 10 mg/kg vinorelbine, the AUC_{0-24} values for *Mdr1a/1b*(−/−) and *Cyp3a*(−/−) mice were 2.3- and 1.5-fold higher than those for WT mice, respectively ($P < 0.01$) (Table 2). However, combined deficiencies of P-gp and Cyp3a resulted in a 1.4-fold lower (rather than higher) AUC_{0-24} than that in WT mice ($P < 0.05$) (Fig. 3B, inset; Table 2). These results suggest that an additional important parameter affecting vinorelbine plasma pharmacokinetics had changed in the *Mdr1a/1b/Cyp3a*(−/−) mice.

Increased Formation of 4′-*O*-Deacetylvinorelbine in *Cyp3a*(−/−) and *Mdr1a/1b/Cyp3a*(−/−) Mice. We have previously observed that the metabolism of midazolam, one of the most widely used probe drugs to assess CYP3A activity, was not reduced in *Cyp3a*(−/−) mice (van Waterschoot et al., 2008). This apparent discrepancy could be attributed to compensatory midazolam metabolism by mouse Cyp2c enzymes, which were substantially up-regulated in *Cyp3a*(−/−) mice (van Waterschoot et al., 2008). We therefore hypothesized that the lower plasma concentrations of vinorelbine in *Mdr1a/1b/Cyp3a*(−/−) mice might also be explained by increased metabolic conversion of vinorelbine, obviously via a metabolic route(s) other than Cyp3a. Because 4′-*O*-deacetylvinorelbine is a major vinorelbine metabolite in mice and humans (van Tellingen et al., 1993; Puozzo et al., 2007), we analyzed the plasma samples from the intravenous experiment for the presence of this metabolite (for the oral experiment, because of the applied multiple sampling approach, the sample size was too small to additionally measure this metabolite). In stark contrast to the parental vinorelbine, plasma concentrations of 4′-*O*-deacetylvinorelbine were highly increased in *Mdr1a/1b/Cyp3a*(−/−) mice compared with those in WT mice (Fig. 3C; Table 2). Of note, single *Cyp3a*(−/−) mice also displayed markedly elevated plasma concentrations of this metabolite. The intravenous AUC_{0-24} for 4′-*O*-deacetylvinorelbine was 3.6-fold higher in *Mdr1a/1b*(−/−) mice, 5.1-fold increased in *Cyp3a*(−/−) mice, and 11.2-fold higher in *Mdr1a/1b/Cyp3a*(−/−) mice than that in WT mice, whereas the equivalent changes in parental vinorelbine AUC_{0-24} were 2.3-, 1.5-, and 0.72-fold, respectively (Table 2). In particular, the *Cyp3a*(−/−) and *Mdr1a/1b/Cyp3a*(−/−) mice thus displayed a profound increase in 4′-*O*-deacetylvinorelbine over vinorelbine concentration ratios. This increased vinorelbine conversion might lead to an underestimation of the effect of the knocked out proteins on vinorelbine clearance.

To determine the additive plasma exposure to vinorelbine and 4′-*O*-deacetylvinorelbine after intravenous vinorelbine, we plotted the combined plasma concentration-time curves and calculated the combined AUC_{0-24} and C_{max} values (Fig. 3D; Table 2). This calculation indicated that the combined

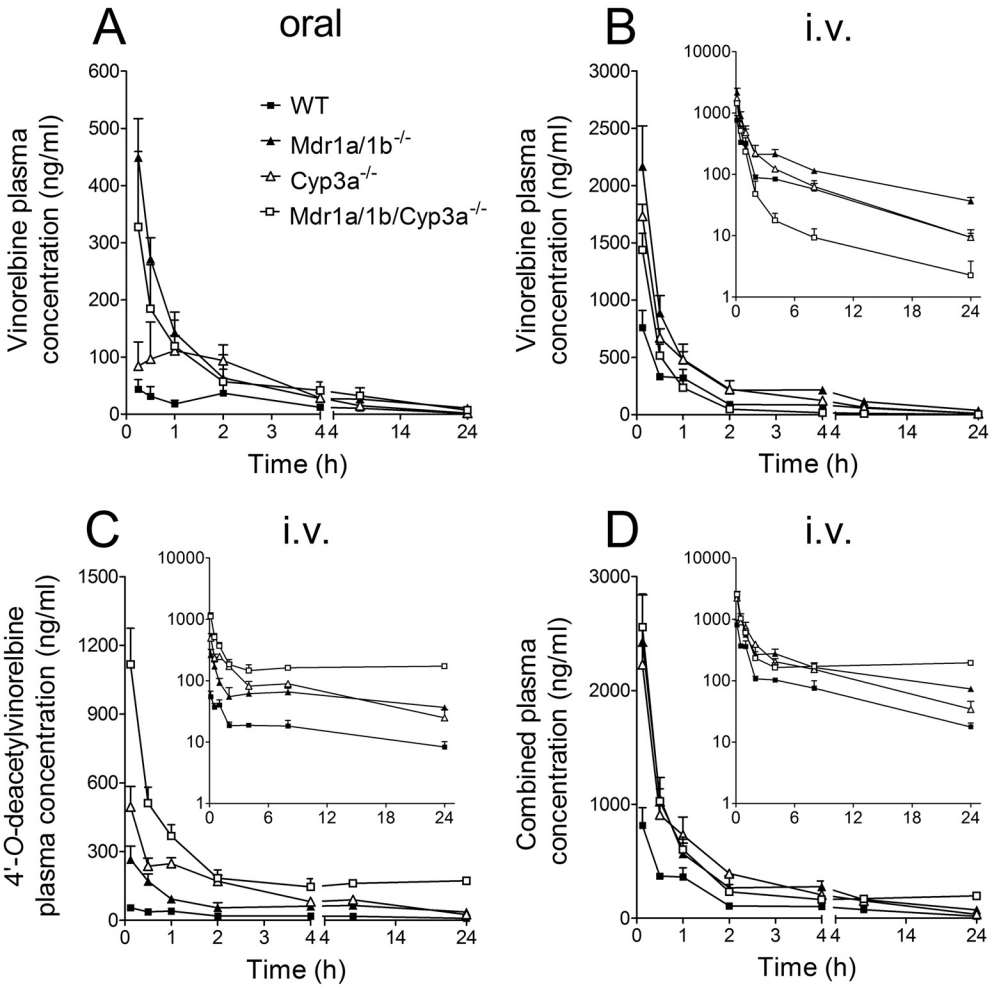

Fig. 3. Plasma concentration-time curves of vinorelbine (A and B), 4′-*O*-deacetylvinorelbine (C) and vinorelbine + 4′-*O*-deacetylvinorelbine (combined; D) in WT (■), *Mdr1a/1b*(−/−) (▲), *Cyp3a*(−/−) (△), and *Mdr1a/1b/Cyp3a*(−/−) (□) mice after oral (A) and intravenous (B, C, and D) administration of vinorelbine at a dose of 10 mg/kg. Data represent mean concentrations ± S.D.; $n = 4$ to 6 for oral and $n = 4$ for intravenous administration. Inserts in B, C, and D show semilog plots of the data.

TABLE 2
Plasma pharmacokinetic parameters after oral or intravenous administration of vinorelbine at 10 mg/kg
Data are means ± S.D.; $n = 4$ to 6 for oral and $n = 4$ for intravenous administration.

	Strain			
	WT	*Mdr1a/1b*(−/−)	*Cyp3a*(−/−)	*Mdr1a/1b/Cyp3a*(−/−)
Oral vinorelbine				
AUC_{0-24}, h · mg^{-1} · l^{-1}	0.25 ± 0.10	0.86 ± 0.37*	0.54 ± 0.15*	0.84 ± 0.22*
C_{max}, mg/l	0.04 ± 0.02	0.45 ± 0.07**	0.11 ± 0.03*	0.33 ± 0.13*
T_{max}, h	0.25	0.25	1	0.25
Intravenous vinorelbine				
AUC_{0-24}, h · mg^{-1} · l^{-1}	1.62 ± 0.27	3.70 ± 0.35**	2.50 ± 0.14**	1.17 ± 0.04*
C_{max}, mg/l	6.30 ± 0.97	2.72 ± 0.24**	4.01 ± 0.23**	8.55 ± 0.31**
T_{max}, h	15.4 ± 6.7	23.2 ± 10.2	21.6 ± 6.1	71.8 ± 19.1*
Intravenous 4′-*O*-deacetylvinorelbine				
AUC_{0-24}, h · mg^{-1} · l^{-1}	0.40 ± 0.05	1.45 ± 0.14**	2.02 ± 0.02**	4.46 ± 0.31**
C_{max}, mg/l				
T_{max}, h	2.01 ± 0.30	5.15 ± 0.46**	4.52 ± 0.14**	5.63 ± 0.29**
$AUC_{i.v.}$ 4′-*O*-deacetylvinorelbine/$AUC_{i.v.}$ vinorelbine				
Exposure ratio	0.25	0.39	0.81	3.8

*$P < 0.05$, compared with WT mice.
**$P < 0.01$.

AUC_{0-24} values were 2.2- to 2.8-fold increased in each of the three knockout strains compared with those in the WT mice, illustrating a markedly reduced elimination of vinorelbine/4′-*O*-deacetylvinorelbine in each of the knockout strains. Still, the overall effect seen in the combination knockout strain was less than expected from the effects seen in the separate knockout strains. 4′-*O*-Deacetylvinorelbine/vinorelbine exposure ratios increased from 0.25 in WT mice to 0.39, 0.81, and 3.8 in *Mdr1a/1b*(−/−), *Cyp3a*(−/−), and *Mdr1a/1b/Cyp3a*(−/−) mice, respectively, suggesting pronounced changes mainly in the latter two strains.

4′-*O*-Deacetylvinorelbine Formation is Up-Regulated in *Cyp3a*(−/−) Liver Microsomes. These results raised the question to what extent vinorelbine in mice is cleared by Cyp3a or perhaps Cyp2c, by conversion to 4′*O*-deacetylvinorelbine, and/or by some other metabolic path-

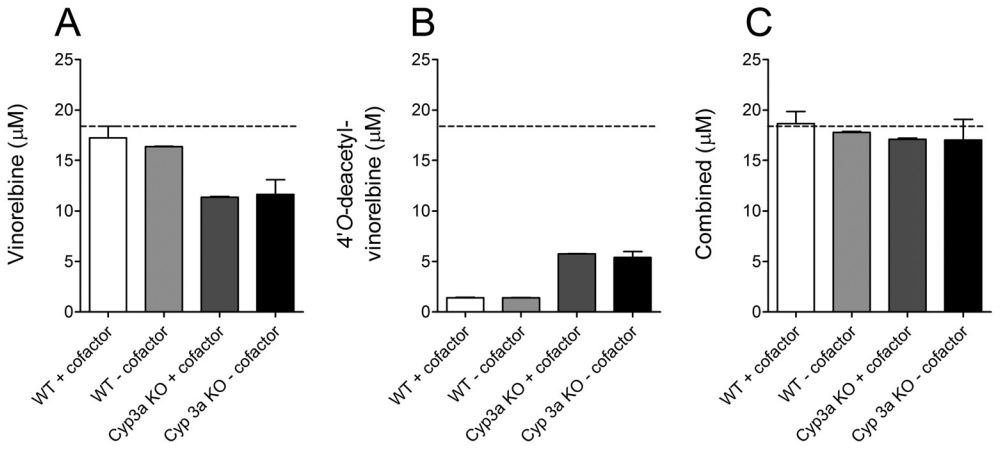

Fig. 4. Concentrations of vinorelbine (A), 4′-*O*-deacetylvinorelbine (B), and vinorelbine + 4′-*O*-deacetylvinorelbine (C; combined) after incubation of liver microsomes from WT or *Cyp3a*(−/−) mice [Cyp3a knockout (KO)] with 18.5 μM vinorelbine for 20 min in the absence or presence of NADPH cofactor. Data represent mean concentrations ± S.D.; $n = 3$. Dashed lines in the three panels represent the applied vinorelbine concentration of 18.5 μM at $t = 0$.

way. Because metabolic drug clearance after intravenous administration is often mostly mediated by the liver, we incubated vinorelbine with liver microsomes from WT and *Cyp3a*(−/−) mice. We assessed P450-mediated metabolism by comparing vinorelbine concentrations in the presence and absence of the cofactor NADPH, which is essential for Cyp activity. In addition, we measured 4′-*O*-deacetylvinorelbine formation. We observed, unexpectedly, only minimal disappearance of vinorelbine in microsomes from WT mice, and the absence or presence of NADPH did not affect this process, indicating that this process was not P450-mediated (Fig. 4A). A small amount of 4′-*O*-deacetylvinorelbine was formed, and this was again not NADPH-dependent (Fig. 4B). In the *Cyp3a*(−/−) microsomes, however, we observed much more extensive disappearance of vinorelbine, correlating with a higher production of 4′-*O*-deacetylvinorelbine (Fig. 4, A and B). Again, these conversions were independent of the presence or absence of NADPH, indicating that they were not P450-mediated. The sum of the remaining vinorelbine and 4′-*O*-deacetylvinorelbine amounts in the various incubations (Fig. 4C) yielded total drug amounts that were not substantially below the originally applied amount of vinorelbine (18.5 μM), suggesting that there was little metabolism to other compounds under these conditions.

Increased 4′-*O*-Deacetylvinorelbine Formation in *Cyp3a*(−/−) and *Mdr1a/1b/Cyp3a*(−/−) Plasma. Because the abundant 4′-*O*-deacetylvinorelbine formation in the *Cyp3a*(−/−) liver microsomes was not P450-mediated, it might be catalyzed by (partly) soluble proteins that could also be secreted into the blood. We therefore incubated vinorelbine (6.5 μM or approximately 5000 ng/ml, i.e., of the same order as expected shortly after intravenous administration of vinorelbine) in vitro with plasma freshly collected from WT, *Mdr1a/1b*(−/−), *Cyp3a*(−/−), and *Mdr1a/1b/Cyp3a*(−/−) mice and measured disappearance of vinorelbine and appearance of 4′-*O*-deacetylvinorelbine over time. In WT and *Mdr1a/1b*(−/−) plasma there was a slow disappearance of vinorelbine, associated with low production of 4′-*O*-deacetylvinorelbine over time (Fig. 5, A and B). Of interest, however, in *Cyp3a*(−/−) plasma, vinorelbine disappearance and 4′-*O*-deacetylvinorelbine appearance were clearly increased, and both processes were markedly further enhanced in the *Mdr1a/1b/Cyp3a*(−/−) plasma. These results indicate that there is substantial up-regulation of enzyme(s) forming 4′-*O*-deacetylvinorelbine in *Cyp3a*(−/−) and especially *Mdr1a/1b/Cyp3a*(−/−) plasma, but not in *Mdr1a/1b*(−/−) plasma. Adding up the vinorelbine plus 4′-*O*-deacetylvinorelbine values in plasma for each strain (Fig. 5C) indicated that most of the drug was still detectable in these two forms after 120 min, suggesting only little metabolism to alternative vinorelbine metabolites.

Up-Regulation of Carboxylesterases in Livers of *Mdr1a/1b*(−/−), *Cyp3a*(−/−), and *Mdr1a/1b/Cyp3a*(−/−) Mice. The conversion of vinorelbine to 4′-*O*-deacetylvinorelbine is essentially an esterase reaction, so we considered that one or more (carboxyl)esterases or paraoxonases produced in the liver and secreted into the blood might be up-regulated in the *Cyp3a*(−/−) and *Mdr1a/1b/Cyp3a*(−/−) strains but not in the *Mdr1a/1b*(−/−) mice. We therefore tested gene expression of all obvious candidate hepatic carboxylesterases (Holmes et al., 2010) and paraoxonases in liver of the different mouse strains using RT-PCR (Supplemental Fig. 1; Supplemental Table 1). The paraoxonase enzymes (Pon1, Pon2, and Pon3) were not differentially expressed in the WT and

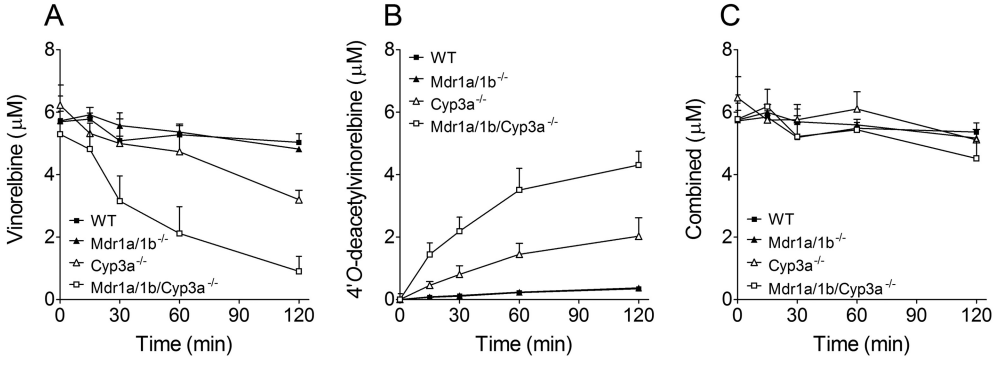

Fig. 5. Concentration-time curves of vinorelbine (A), 4′-*O*-deacetylvinorelbine (B), and vinorelbine + 4′-*O*-deacetylvinorelbine (C; combined) after ex vivo incubation of 6.5 μM vinorelbine in plasma of WT (■), *Mdr1a/1b*(−/−) (▲), *Cyp3a*(−/−) (△), and *Mdr1a/1b/Cyp3a*(−/−) (□) mice. Data represent mean concentrations ± S.D.; $n = 4$.

knockout strains. In contrast, four (Ces1b, Ces1c, Ces1d, and Ces1e) of the six Ces1 enzymes tested were found to be highly up-regulated in all three knockout strains. However, because these genes were also up-regulated to the same extent in *Mdr1a/1b*(−/−) mice, whereas metabolite formation in *Mdr1a/1b*(−/−) mice was similar to that in WT mice (Fig. 5), these Ces1 enzymes cannot be responsible for the (increased) formation of 4′-*O*-deacetylvinorelbine. Of interest, however, the carboxylesterase Ces2a (formerly named Ces6) was 2.7-fold up-regulated in *Cyp3a*(−/−) and 3.9-fold in *Mdr1a/1b/Cyp3a*(−/−) mice, whereas its expression was not altered in *Mdr1a/1b*(−/−) mice (Fig. 6D; Supplemental Fig. 1; Supplemental Table 1). On the basis of this Ces2a expression pattern (Fig. 6D) and its similarity to the pattern of metabolite formation in the knockout strains (Figs. 5 and 6, A–C), Ces2a is the only plausible carboxylesterase candidate for the increased formation of 4′-*O*-deacetylvinorelbine.

Increased 4′-*O*-Deacetylvinorelbine Formation Can Be Inhibited by BNPP and Loperamide. To further corroborate the involvement of carboxylesterases and especially Ces2a, we tested whether the formation of 4′-*O*-deacetylvinorelbine in plasma could be inhibited using the nonspecific carboxylesterase inhibitor BNPP and the (human) CES2-specific inhibitor loperamide (Wang et al., 2011; Williams et al., 2011). We incubated vinorelbine (6.5 μM) with BNPP (100 μM), loperamide (100 μM), or vehicle for 120 min in vitro with plasma freshly collected from WT, *Mdr1a/1b*(−/−), *Cyp3a*(−/−), and *Mdr1a/1b/Cyp3a*(−/−) mice, and we measured disappearance of vinorelbine and appearance of 4′-*O*-deacetylvinorelbine over time. Loperamide inhibited the formation of 4′-*O*-deacetylvinorelbine approximately 2- to 3-fold in all four strains, whereas BNPP completely inhibited metabolite formation (Fig. 6, A and B). Adding up the vinorelbine plus 4′-*O*-deacetylvinorelbine values in plasma for each strain (Fig. 6C) suggested little metabolism to alternative vinorelbine metabolites. Moreover, we obtained similar inhibition data with liver microsomes of WT and Cyp3a knockout mice (Supplemental Fig. 2). In microsomes of *Cyp3a*(−/−) mice, loperamide inhibited the formation of 4′-*O*-deacetylvinorelbine ~3-fold, whereas BNPP completely inhibited metabolite formation. Taken together, these inhibition results combined with the RNA expression data indicate that a carboxylesterase is responsible for the formation of 4′-*O*-deacetylvinorelbine in liver and plasma and that this carboxylesterase is most likely Ces2a.

Discussion

In this study, we demonstrated that vinorelbine is a transported substrate for MRP2 and that loss of Mrp2 in mice resulted in a 1.5-fold elevated plasma exposure upon oral vinorelbine administration. The absence of P-gp in mice resulted in a marked (~3.5-fold) increase in plasma exposure after oral vinorelbine and a 2.3-fold increase after intravenous vinorelbine. The absence of Cyp3a alone or combined absence of P-gp and Cyp3a also resulted in increased plasma exposure levels (2.2- and 3.4-fold, respectively) of oral vinorelbine. However, these latter values are probably an underestimate, as in both strains, especially the *Mdr1a/1b/Cyp3a*(−/−) mice (and in contrast to the single P-gp-deficient strain), there was a substantial up-regulation of plasma enzyme(s) that convert vinorelbine to its major metabolite 4′-*O*-deacetylvinorelbine. The impact of this up-regulation was even more apparent after intravenous vinorelbine administration. Inhibition experiments together with RT-PCR expression data indicated that up-regulation of Ces2a is most

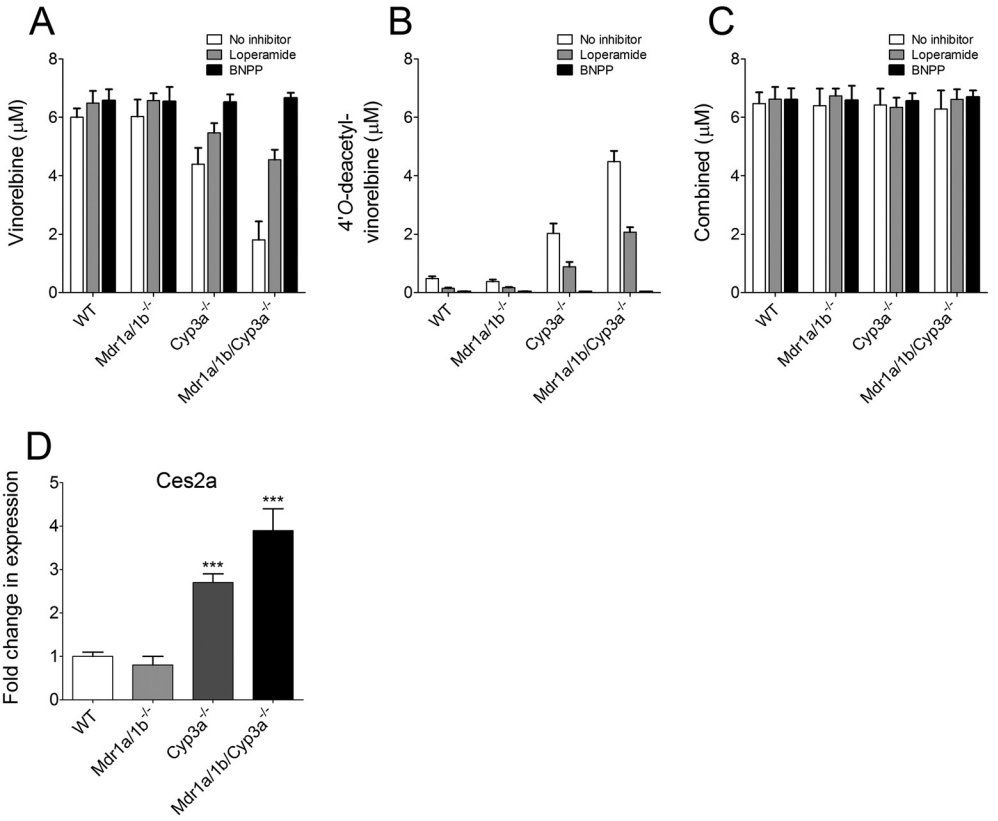

Fig. 6. Concentrations of vinorelbine (A), 4′-*O*-deacetylvinorelbine (B), and vinorelbine + 4′-*O*-deacetylvinorelbine (C; combined) after ex vivo incubation of 6.5 μM vinorelbine for 120 min in plasma of WT, *Mdr1a/1b*(−/−), *Cyp3a*(−/−), and *Mdr1a/1b/Cyp3a*(−/−) mice in the absence or presence of the nonspecific carboxylesterase inhibitor BNPP (100 μM) or the CES2-specific inhibitor loperamide (100 μM). Data represent mean concentrations ± SD; $n = 3$. D, expression levels of Ces2a in livers of WT, *Mdr1a/1b*(−/−), *Cyp3a*(−/−), and *Mdr1a/1b/Cyp3a*(−/−) mice, as determined by real-time RT-PCR. Data are normalized to glyceraldehyde-3-phosphate dehydrogenase expression. Values represent mean fold change ± SD, compared with WT mice; $n = 3$. ***, $P < 0.001$, compared with WT ΔCt values.

likely responsible for the (increased) formation of 4′*O*-deacetylvinorelbine in the *Cyp3a*(−/−) and *Mdr1a/1b/Cyp3a*(−/−) mice.

Thus far, interactions of vinorelbine with MRP2 have not been reported. However, cellular resistance to the vinca alkaloid vincristine has been associated with MRP2 expression (Chen et al., 1999; Kawabe et al., 1999), and transport of vinblastine by MRP2 has been demonstrated in vitro (Evers et al., 1998, 2000a; Huisman et al., 2005). In this study, we show that human MRP2 can efficiently transport vinorelbine in vitro. This very likely means that tumor cells expressing this protein will to some extent be protected from the cytotoxicity of vinorelbine. Moreover, *Mrp2*(−/−) mice had significantly higher plasma vinorelbine concentrations than WT mice, especially at early time points (15 and 30 min) after oral administration, suggesting that Mrp2 can limit the intestinal uptake of vinorelbine. This could also mean that MRP2 activity and variations in its expression or activity level in patients due to genetic polymorphisms or induction or inhibition by other coadministered drugs may affect the therapeutic efficacy of vinorelbine.

The marked (3.5-fold) increase in plasma exposure after oral vinorelbine in *Mdr1a/1b*(−/−) mice indicates that P-gp is an important determinant of oral availability of vinorelbine. The increase in plasma levels was especially evident shortly after vinorelbine administration, suggesting that the intestinal uptake was improved. Although vinorelbine is an established P-gp substrate (Adams and Knick, 1995; Shepard et al., 2003), in contrast to our results, it was previously reported that *Mdr1a/1b*(−/−) mice did not have a statistically significantly increased plasma AUC upon oral vinorelbine administration at 10 mg/kg (Press et al., 2006). However, variation in plasma levels in those experiments was extremely high, hampering reliable comparisons between strains. We have since then found that the reproducibility of plasma levels upon oral drug administration to mice can be markedly improved by including a short (3 h) fasting period before administration, and this was applied in the vinorelbine experiments described in the current study. Press et al. (2006) did find a clear and highly significant reduction in fecally excreted vinorelbine in *Mdr1a/1b*(−/−) mice (from 34 to 6% of the dose), in line with a role of P-gp in limiting intestinal uptake of vinorelbine (Press et al., 2006). Taken together, our results show that P-gp appears to substantially limit the oral availability of vinorelbine in mice. Because vinorelbine is also a good substrate of human P-gp, this might also contribute to the variable oral availability of vinorelbine in patients. The previously reported association in patients of low intravenous vinorelbine clearance and low apparent P-gp clearance activity (Wong et al., 2006) is also in line with our findings in *Mdr1a/1b*(−/−) mice. Possibly inhibiting P-gp with a dedicated modulating drug might therefore improve the oral and intravenous availability and overall therapeutic efficacy of vinorelbine in patients.

The interpretation of vinorelbine experiments in the *Cyp3a*(−/−) and *Mdr1a/1b/Cyp3a*(−/−) mice is complicated by the marked up-regulation of the plasma and liver carboxylesterase enzyme that converts vinorelbine to 4′*O*-deacetylvinorelbine. This almost certainly means that the vinorelbine AUCs measured in these strains for vinorelbine are an underestimate of the values that would have occurred without this up-regulation. Despite this, the oral and intravenous AUCs of vinorelbine were still significantly (2.2- and 1.5-fold, respectively) increased in *Cyp3a*(−/−) mice relative to those in WT mice. This finding strongly suggests that Cyp3a-mediated metabolism does substantially reduce the effective availability of vinorelbine, consistent with the previous demonstration that CYP3A4 and, to a lesser extent, CYP3A5 are the primary vinorelbine-metabolizing enzymes in human liver microsomes, although the various metabolites formed have not been structurally defined yet (Kajita et al., 2000; Beulz-Riche et al., 2005). In combination with our mouse data, this also suggests that CYP3A4 and CYP3A5 may affect the oral and intravenous availability of vinorelbine in humans. These enzymes can display substantial inter- and intraindividual variation in expression and they are involved in many drug-drug interactions by either gene induction or direct inhibition, which could affect the therapeutic efficacy of vinorelbine.

We note that metabolism of vinorelbine by soluble (plasma) enzymes was thus far not tested (Kajita et al., 2000; Beulz-Riche et al., 2005). However, 4′-*O*-deacetylvinorelbine is a major vinorelbine metabolite found in both mouse and human plasma, and this metabolite is also pharmacodynamically active (van Tellingen et al., 1993; Briasoulis et al., 2009). It is therefore interesting to find that one (or more) plasma enzyme(s) can mediate substantial formation of this metabolite. It has previously been suggested that 4′-*O*-deacetylvinorelbine is formed by a carboxylesterase, but its identity has thus far not been resolved (e.g., Delord et al., 2009). In this study we have been able to identify mouse Ces2a as the most likely candidate for 4′-*O*-deacetylvinorelbine formation. We note that loperamide is a specific CES2 inhibitor with $IC_{50} = \leq 1$ μM in humans, $IC_{50} = \sim 100$ μM for dog, and $IC_{50} = \sim 35$ μM for monkey (Williams et al., 2011). For mouse Ces2a, IC_{50} values for loperamide have thus far not been reported, but our results of ~50% inhibition at a concentration of 100 μM are well in line with the IC_{50} values obtained in other animal species. Further experiments with recombinant mouse Ces2a, which is currently not available to us, could clarify these results further.

The up-regulation of Ces2a makes it difficult to interpret the combined effect of P-gp and Cyp3a deficiency in the *Mdr1a/1b/Cyp3a*(−/−) mice on vinorelbine availability, after either oral or intravenous drug administration. Presumably, without this up-regulation, the AUC of vinorelbine would have been considerably higher than that in the separate *Mdr1a/1b*(−/−) or *Cyp3a*(−/−) mice. This problem cannot be solved by considering the sum of vinorelbine and 4′*O*-deacetylvinorelbine, because the further disposition and metabolism of either compound might be quite different. Any statement on the possible interaction between Cyp3a and Mdr1a/1b P-gp affecting vinorelbine availability therefore remains speculative. These findings once again illustrate that great caution should be exercised in the assessment of pharmacokinetic and related effects in knockout mouse strains, as there can sometimes be important changes in alternative detoxification pathways. This seems to be especially a risk with Cyp3a-deficient mouse strains (van Waterschoot et al., 2008 and the present study), although in the present study we also found up-regulation of some carboxylesterase genes in *Mdr1a/1b*(−/−) mice.

In summary, we have demonstrated a substantial in vivo impact of P-gp, Mrp2, and Cyp3a on vinorelbine availability

and clearance in mice, as well as the involvement of a plasma carboxylesterase, most likely Ces2a. Variation in the activity of their human homologs is also likely to affect vinorelbine pharmacokinetics and therapeutic efficacy in patients.

Acknowledgments

We acknowledge Dr. Olaf van Tellingen (The Netherlands Cancer Institute) for help with the synthesis of 4′-*O*-deacetylvinorelbine, which was used in the LC-MS/MS assay (Damen et al., 2009). We are grateful to Anita van Esch (The Netherlands Cancer Institute) for RT-PCR analysis and to Dr. Hilde Rosing and Abadi Gebretensae (Slotervaart Hospital) for LC-MS/MS analysis.

Authorship Contributions

Participated in research design: Lagas, Damen, van Waterschoot, and Schinkel.

Conducted experiments: Lagas, Damen, van Waterschoot, and Iusuf.

Contributed new reagents or analytic tools: Beijnen.

Performed data analysis: Lagas, Damen, Iusuf, and Schinkel.

Wrote or contributed to the writing of the manuscript: Lagas and Schinkel.

References

Abraham J, Edgerly M, Wilson R, Chen C, Rutt A, Bakke S, Robey R, Dwyer A, Goldspiel B, Balis F, et al. (2009) A phase I study of the P-glycoprotein antagonist tariquidar in combination with vinorelbine. *Clin Cancer Res* **15:**3574–3582.

Adams DJ and Knick VC (1995) P-glycoprotein mediated resistance to 5′-noranhydro-vinblastine (Navelbine). *Invest New Drugs* **13:**13–21.

Beulz-Riché D, Grudé P, Puozzo C, Sautel F, Filaquier C, Riché C, and Ratanasavanh D (2005) Characterization of human cytochrome P450 isoenzymes involved in the metabolism of vinorelbine. *Fundam Clin Pharmacol* **19:**545–553.

Briasoulis E, Pappas P, Puozzo C, Tolis C, Fountzilas G, Dafni U, Marselos M, and Pavlidis N (2009) Dose-ranging study of metronomic oral vinorelbine in patients with advanced refractory cancer. *Clin Cancer Res* **15:**6454–6461.

Chen ZS, Kawabe T, Ono M, Aoki S, Sumizawa T, Furukawa T, Uchiumi T, Wada M, Kuwano M, and Akiyama SI (1999) Effect of multidrug resistance-reversing agents on transporting activity of human canalicular multispecific organic anion transporter. *Mol Pharmacol* **56:**1219–1228.

Damen CW, Lagas JS, Rosing H, Schellens JH, and Beijnen JH (2009) The bioanalysis of vinorelbine and 4-*O*-deacetylvinorelbine in human and mouse plasma using high-performance liquid chromatography coupled with heated electrospray ionization tandem mass-spectrometry. *Biomed Chromatogr* **23:**1316–1325.

Delord JP, Puozzo C, Lefresne F, and Bugat R (2009) Combination chemotherapy of vinorelbine and cisplatin: a phase I pharmacokinetic study in patients with metastatic solid tumors. *Anticancer Res* **29:**553–560.

Domenech GH and Vogel CL (2001) A review of vinorelbine in the treatment of breast cancer. *Clin Breast Cancer* **2:**113–128.

Emoto C, Yamazaki H, Yamasaki S, Shimada N, Nakajima M, and Yokoi T (2000) Characterization of cytochrome P450 enzymes involved in drug oxidations in mouse intestinal microsomes. *Xenobiotica* **30:**943–953.

Evers R, de Haas M, Sparidans R, Beijnen J, Wielinga PR, Lankelma J, and Borst P (2000a) Vinblastine and sulfinpyrazone export by the multidrug resistance protein MRP2 is associated with glutathione export. *Br J Cancer* **83:**375–383.

Evers R, Kool M, Smith AJ, van Deemter L, de Haas M, and Borst P (2000b) Inhibitory effect of the reversal agents V-104, GF120918 and Pluronic L61 on MDR1 Pgp-, MRP1- and MRP2-mediated transport. *Br J Cancer* **83:**366–374.

Evers R, Kool M, van Deemter L, Janssen H, Calafat J, Oomen LC, Paulusma CC, Oude Elferink RP, Baas F, Schinkel AH, et al. (1998) Drug export activity of the human canalicular multispecific organic anion transporter in polarized kidney MDCK cells expressing cMOAT (MRP2) CDNA. *J Clin Invest* **101:**1310–1319.

Gralla RJ, Gatzemeier U, Gebbia V, Huber R, O'Brien M, and Puozzo C (2007) Oral vinorelbine in the treatment of non-small cell lung cancer: rationale and implications for patient management. *Drugs* **67:**1403–1410.

Hirsh V, Desjardins P, Needles BM, Rigas JR, Jahanzeb M, Nguyen L, Zembryki D, and Leopold LH (2007) Oral versus intravenous administration of vinorelbine as a single agent for the first-line treatment of metastatic nonsmall cell lung carcinoma (NSCLC): a randomized phase II trial. *Am J Clin Oncol* **30:**245–251.

Holmes RS, Wright MW, Laulederkind SJ, Cox LA, Hosokawa M, Imai T, Ishibashi S, Lehner R, Miyazaki M, Perkins EJ, et al. (2010) Recommended nomenclature for five mammalian carboxylesterase gene families: human, mouse, and rat genes and proteins. *Mamm Genome* **21:**427–441.

Huisman MT, Chhatta AA, van Tellingen O, Beijnen JH, and Schinkel AH (2005) MRP2 (ABCC2) transports taxanes and confers paclitaxel resistance and both processes are stimulated by probenecid. *Int J Cancer* **116:**824–829.

Irvine JD, Takahashi L, Lockhart K, Cheong J, Tolan JW, Selick HE, and Grove JR (1999) MDCK (Madin-Darby canine kidney) cells: a tool for membrane permeability screening. *J Pharm Sci* **88:**28–33.

Kajita J, Kuwabara T, Kobayashi H, and Kobayashi S (2000) CYP3A4 is mainly responsibile for the metabolism of a new vinca alkaloid, vinorelbine, in human liver microsomes. *Drug Metab Dispos* **28:**1121–1127.

Kawabe T, Chen ZS, Wada M, Uchiumi T, Ono M, Akiyama S, and Kuwano M (1999) Enhanced transport of anticancer agents and leukotriene C4 by the human canalicular multispecific organic anion transporter (CMOAT/MRP2). *FEBS Lett* **456:**327–331.

Lê LH, Moore MJ, Siu LL, Oza AM, MacLean M, Fisher B, Chaudhary A, de Alwis DP, Slapak C, and Seymour L (2005) Phase I study of the multidrug resistance inhibitor zosuquidar administered in combination with vinorelbine in patients with advanced solid tumours. *Cancer Chemother Pharmacol* **56:**154–160.

Marty M, Fumoleau P, Adenis A, Rousseau Y, Merrouche Y, Robinet G, Senac I, and Puozzo C (2001) Oral vinorelbine pharmacokinetics and absolute bioavailability study in patients with solid tumors. *Ann Oncol* **12:**1643–1649.

Press RR, Buckle T, Beijnen JH, and van Tellingen O (2006) The effect of P-glycoprotein and cytochrome P450 3a on the oral bioavailability of vinorelbine in mice. *Cancer Chemother Pharmacol* **57:**819–825.

Puozzo C, Ung HL, and Zorza G (2007) A high performance liquid chromatography method for vinorelbine and 4-*O*-deacetyl vinorelbine: a decade of routine analysis in human blood. *J Pharm Biomed Anal* **44:**144–149.

Rossi D, Catalano V, Alessandroni P, Fedeli A, Fedeli SL, Giordani P, Baldelli AM, Casadei V, Ceccolini M, Ugolini M, et al. (2007) A phase II study of single-agent oral vinorelbine in patients with pretreated advanced non-small-cell lung cancer. *Clin Lung Cancer* **8:**382–385.

Schinkel AH, Mayer U, Wagenaar E, Mol CA, van Deemter L, Smit JJ, van der Valk MA, Voordouw AC, Spits H, van Tellingen O, et al. (1997) Normal viability and altered pharmacokinetics in mice lacking Mdr1-type (drug-transporting) P-glycoproteins. *Proc Natl Acad Sci USA* **94:**4028–4033.

Schinkel AH, Wagenaar E, van Deemter L, Mol CA, and Borst P (1995) Absence of the Mdr1a P-glycoprotein in mice affects tissue distribution and pharmacokinetics of dexamethasone, digoxin, and cyclosporin A. *J Clin Invest* **96:**1698–1705.

Schmittgen TD and Livak KJ (2008) Analyzing real-time PCR data by the comparative C_T method. *Nat Protoc* **3:**1101–1108.

Shepard RL, Cao J, Starling JJ, and Dantzig AH (2003) Modulation of P-glycoprotein but not MRP1- or BCRP-mediated drug resistance by LY335979. *Int J Cancer* **103:**121–125.

Takara K, Sakaeda T, Yagami T, Kobayashi H, Ohmoto N, Horinouchi M, Nishiguchi K, and Okumura K (2002) Cytotoxic effects of 27 anticancer drugs in HeLa and MDR1-overexpressing derivative cell lines. *Biol Pharm Bull* **25:**771–778.

van Herwaarden AE, Wagenaar E, van der Kruijssen CM, van Waterschoot RA, Smit JW, Song JY, van der Valk MA, van Tellingen O, van der Hoorn JW, Rosing H, et al. (2007) Knockout of cytochrome P450 3A yields new mouse models for understanding xenobiotic metabolism. *J Clin Invest* **117:**3583–3592.

van Tellingen O, Kuijpers A, Beijnen JH, Baselier MR, Burghouts JT, and Nooyen WJ (1992) Bio-analysis of vinorelbine by high-performance liquid chromatography with fluorescence detection. *J Chromatogr* **573:**328–332.

van Tellingen O, Kuijpers AV, Beijnen JH, Nooijen WJ, and Bult A (1993) Plasma pharmacokinetics, tissue disposition, excretion and metabolism of vinorelbine in mice as determined by high performance liquid chromatography. *Invest New Drugs* **11:**141–150.

van Waterschoot RA, Lagas JS, Wagenaar E, van der Kruijssen CM, van Herwaarden AE, Song JY, Rooswinkel RW, van Tellingen O, Rosing H, Beijnen JH, et al. (2009) Absence of both cytochrome P450 3A and P-glycoprotein dramatically increases docetaxel oral bioavailability and risk of intestinal toxicity. *Cancer Res* **69:**8996–9002.

van Waterschoot RA, van Herwaarden AE, Lagas JS, Sparidans RW, Wagenaar E, van der Kruijssen CM, Goldstein JA, Zeldin DC, Beijnen JH, and Schinkel AH (2008) Midazolam metabolism in cytochrome P450 3A knockout mice can be attributed to up-regulated CYP2C enzymes. *Mol Pharmacol* **73:**1029–1036.

Vlaming ML, Mohrmann K, Wagenaar E, de Waart DR, Elferink RP, Lagas JS, van Tellingen O, Vainchtein LD, Rosing H, Beijnen JH, et al. (2006) Carcinogen and anticancer drug transport by Mrp2 in vivo: studies using Mrp2 (Abcc2) knockout mice. *J Pharmacol Exp Ther* **318:**319–327.

Wang J, Williams ET, Bourgea J, Wong YN, and Patten CJ (2011) Characterization of recombinant human carboxylesterases: fluorescein diacetate as a probe substrate for human carboxylesterase 2. *Drug Metab Dispos* **39:**1329–1333.

Williams ET, Bacon JA, Bender DM, Lowinger JJ, Guo WK, Ehsani ME, Wang X, Wang H, Qian YW, Ruterbories KJ, et al. (2011) Characterization of the expression and activity of carboxylesterases 1 and 2 from the beagle dog, cynomolgus monkey, and human. *Drug Metab Dispos* **39:**2305–2313.

Wong M, Balleine RL, Blair EY, McLachlan AJ, Ackland SP, Garg MB, Evans S, Farlow D, Collins M, Rivory LP, et al. (2006) Predictors of vinorelbine pharmacokinetics and pharmacodynamics in patients with cancer. *J Clin Oncol* **24:**2448–2455.

Yuan JS, Reed A, Chen F, and Stewart CN Jr (2006) Statistical analysis of real-time PCR data. *BMC Bioinformatics* **7:**85.

Address correspondence to: Dr. Jurjen S. Lagas, Department of Pharmacy and Pharmacology, Slotervaart Hospital, Louwesweg 6, 1066 EC Amsterdam, The Netherlands. E-mail: jurjen.lagas@slz.nl